



Revisiting the bilayer structures of fluid phase phosphatidylglycerol lipids: Accounting for exchangeable hydrogens



Jianjun Pan^{a,*}, Drew Marquardt^b, Frederick A. Heberle^c, Norbert Kučerka^{d,e}, John Katsaras^{b,c,f,g,**}

^a Department of Physics, University of South Florida, Tampa, FL 33620, USA

^b Department of Physics, Brock University, St. Catharines, ON L2S 3A1, Canada

^c Neutron Sciences Directorate, Oak Ridge National Laboratory, Oak Ridge, TN 37831, USA

^d Department of Physical Chemistry of Drugs, Comenius University, 832 32 Bratislava, Slovakia

^e Frank Laboratory of Neutron Physics, Joint Institute for Nuclear Research, 141980 Dubna, Russia

^f Joint Institute for Neutron Scattering, Oak Ridge National Laboratory, Oak Ridge, TN 37831, USA

^g Department of Physics and Astronomy, University of Tennessee, Knoxville, TN 37996, USA

ARTICLE INFO

Article history:

Received 17 June 2014

Received in revised form 6 August 2014

Accepted 8 August 2014

Available online 15 August 2014

Keywords:

Lipid bilayer structure

SANS

SAXS

MD simulations

PG lipid

Hydrogen exchange

ABSTRACT

We recently published two papers detailing the structures of fluid phase phosphatidylglycerol (PG) lipid bilayers (Kučerka et al., 2012 J. Phys. Chem. B 116: 232–239; Pan et al., 2012 Biochim. Biophys. Acta Biomembr. 1818: 2135–2148), which were determined using the scattering density profile model. This hybrid experimental/computational technique utilizes molecular dynamics simulations to parse a lipid bilayer into components whose volume probabilities follow simple analytical functional forms. Given the appropriate scattering densities, these volume probabilities are then translated into neutron scattering length density (NSLD) and electron density (ED) profiles, which are used to jointly refine experimentally obtained small angle neutron and X-ray scattering data. However, accurate NSLD and ED profiles can only be obtained if the bilayer's chemical composition is known. Specifically, in the case of neutron scattering, the lipid's exchangeable hydrogens with aqueous D₂O must be accounted for, as they can have a measurable effect on the resultant lipid bilayer structures. This was not done in our above-mentioned papers. Here we report on the molecular structures of PG lipid bilayers by appropriately taking into account the exchangeable hydrogens. Analysis indicates that the temperature-averaged PG lipid areas decrease by 1.5 to 3.8 Å², depending on the lipid's acyl chain length and unsaturation, compared to PG areas when hydrogen exchange was not taken into account.

© 2014 Elsevier B.V. All rights reserved.

1. Introduction

Lipid membranes play important roles in biological systems [1–4]. Because of this, solving the structures of fully hydrated lipid bilayers has been a longstanding goal of membrane biophysics [5–13]. In the case of biologically relevant membranes, thermal fluctuations preclude the determination of individual atomic positions [14,15]. Lipid bilayer structures are thus best described by statistical averages of atomic

groups which exhibit similar characteristics, for example scattering density. Indeed, X-ray and neutron scattering have been extensively used to elucidate the average structures of flexible lipid bilayers [16–19]. However, each technique is only capable of resolving specific features of the bilayer. For example, X-ray scattering is sensitive to the headgroup's electron dense phosphate moiety [20,21], whereas neutron scattering is better suited to revealing the position of the glycerol/carbonyl backbone – due to its lack of hydrogen atoms. To exploit the strengths of each technique, the matter density-based scattering density profile (SDP) model was developed [22], which allows for the joint refinement of the different contrast neutron and X-ray data, as well as the inclusion of independently obtained volumetric data. However, SDP analysis requires that the bilayer's chemical composition is known. Specifically, in the case of neutron scattering, neutrons “see” deuterium (D) atoms (the heavy, stable isotope of hydrogen) very differently than they do hydrogen (H) atoms, as the coherent neutron scattering lengths for H and D atoms differ substantially in both phase and magnitude.

The terminal glycerol of phosphatidylglycerol (PG) lipids contains two OH groups which are capable of fast hydrogen exchange with the surrounding solvent, as demonstrated by nuclear magnetic resonance

Abbreviations: SDP, scattering density profile; SANS, small angle neutron scattering; SAXS, small angle X-ray scattering; MD, molecular dynamics; NSLD, neutron scattering length density; ED, electron density; vP, volume probability; PG, phosphatidylglycerol; DOPG, 1,2-dioleoyl-*sn*-glycero-3-phosphatidylglycerol; POPG, 1-palmitoyl-2-oleoyl-*sn*-glycero-3-phosphatidylglycerol; SOPG, 1-stearoyl-2-oleoyl-*sn*-glycero-3-phosphatidylglycerol; DLPG, 1,2-dilauroyl-*sn*-glycero-3-phosphatidylglycerol; DMPG, 1,2-dimyristoyl-*sn*-glycero-3-phosphatidylglycerol; DPPG, 1,2-dipalmitoyl-*sn*-glycero-3-phosphatidylglycerol; DSPG, 1,2-distearoyl-*sn*-glycero-3-phosphatidylglycerol

* Correspondence to: J.J. Pan, Department of Physics, University of South Florida, Tampa, FL 33620, USA.

** Correspondence to: J. Katsaras, Joint Institute for Neutron Sciences, Oak Ridge National Laboratory, Oak Ridge, TN 37831, USA.

E-mail addresses: panj@usf.edu (J. Pan), katsarasj@ornl.gov (J. Katsaras).

(NMR) studies [23]. The exchange between PG hydrogens and water has a profound effect on the neutron scattering length density (NSLD) of PG bilayers when in contact with water other than pure H₂O (i.e., varying ratios of H₂O/D₂O). It is then obvious that accurate NSLD and electron density (ED) profiles can only be obtained if the bilayer's chemical composition is known, i.e., exchangeable hydrogens are fully accounted for. This was not done in our previously published papers detailing the structures of PG bilayers [24,25]. Here, we report on the molecular structures of PG lipid bilayers, including the effects of exchangeable OH hydrogens. We find that when accounting for exchangeable hydrogens, temperature-averaged PG lipid areas decrease by 1.5 to 3.8 Å², compared to our previous analyses.

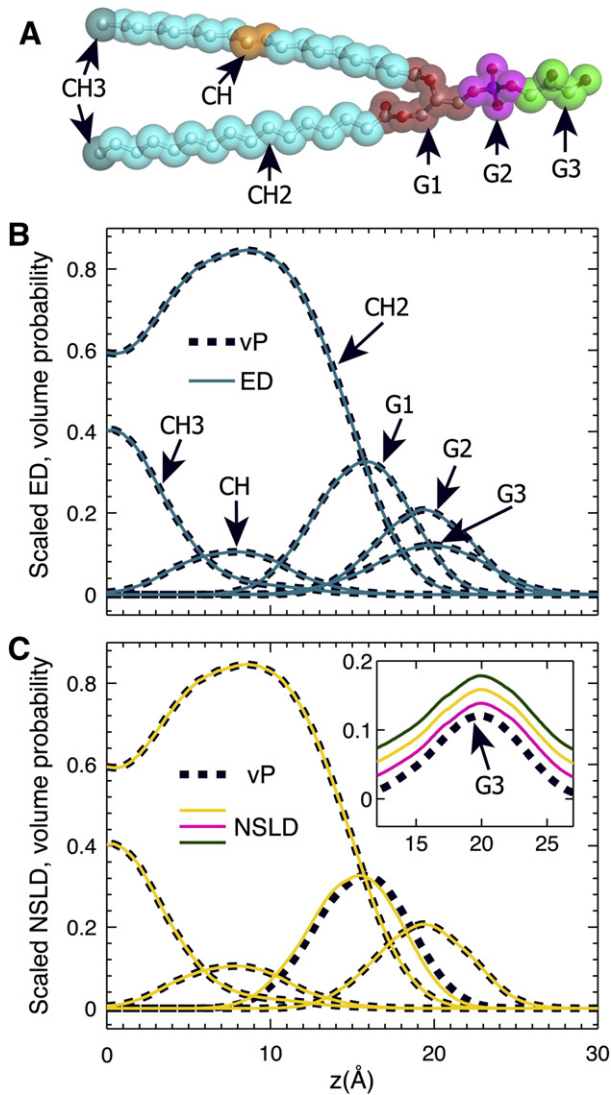


Fig. 1. Comparing component ED and NSLD profiles to their volume probabilities. Three sets of profiles were calculated from *NPT* simulations of a POPG bilayer with an average lipid area of 62.9 Å². (A) Parsing of POPG into six components, each is represented by semi-transparent spheres of different colors. (B) Component EDs (solid cyan lines) were scaled by the ratio of the component volume and electron number. Good overlap was obtained between EDs and the corresponding volume probabilities (vPs, dark dashed lines) for all components. (C) Similar to EDs, component NSLDs (yellow solid lines) were scaled to match their corresponding vPs (dark dashed lines), except in the case of the terminal glycerol (G3). The three G3 NSLDs (inset) were calculated assuming 100% (magenta), 70% (yellow) and 50% (green) deuteration of the two hydroxyls. G3 NSLDs for 50% and 70% OH deuteration are shifted vertically for better visualization when comparing to their vP (dark dashed line). It is clear that each component's NSLD and vP have similar centers and shapes. The only discrepancy is the position of G1, most likely the result of a biased distribution of hydrogens between the interfacial glycerol and backbone carbonyl moieties.

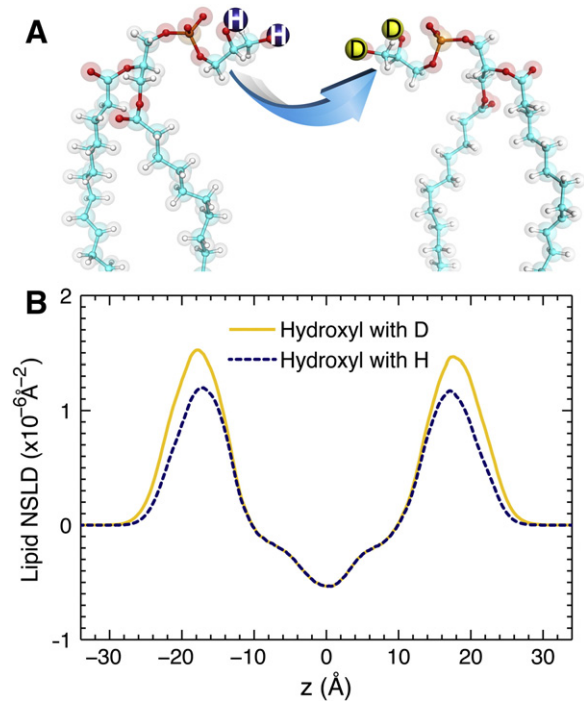


Fig. 2. The effect of hydrogen exchange on the NSLD of POPG. (A) A schematic of hydrogen exchange for the two hydroxyls on the PG headgroup. At 0% D₂O, two hydrogens (blue spheres) are associated with the hydroxyl oxygens. When 100% H₂O is exchanged for 100% D₂O, the two hydroxyl hydrogens are replaced by two deuteriums (yellow spheres). (B) NSLD of a POPG bilayer (water not included). The yellow solid line corresponds to a bilayer with deuterated hydroxyls and the blue dashed line corresponds to a bilayer with protiated hydroxyls. The two profiles were obtained from atom number density distributions (*NPT* simulations with a POPG lipid area of 62.9 Å²) after being multiplied by their corresponding neutron scattering power.

2. Methods

To simultaneously refine small angle X-ray scattering (SAXS) and neutron scattering (SANS) data, an SDP model was developed for PG bilayers [24]. In this model, bilayer hydrocarbon chains were parsed into components made up of terminal methyl (CH₃), methylene (CH₂) and methine (CH) groups, and the headgroup was parsed into components encompassing the glycerol-carbonyl backbone (G1), phosphate (G2) and terminal glycerol (G3) groups (Fig. 1A). Such a parsing scheme enables ED and NSLD component profiles to be commonly described by component volume probability (vP) distributions. An example is shown in Fig. 1B. The dashed lines represent component volume probabilities calculated from constant number, pressure and temperature (*NPT*) simulations of a POPG bilayer with an average lipid area of 62.9 Å². Each component's ED (solid cyan lines) was scaled by the ratio of the component volume and electron number. Good overlap

Table 1

Structural parameters of seven PG lipid bilayers obtained from SDP analysis, where hydrogen exchange with solvent deuterium was accounted for. The units for lipid area *A*, overall bilayer thickness *D_B*, and hydrocarbon thickness *2D_C* are in Å², Å and Å, respectively. The estimated uncertainty for each parameter is ~2%.

	20 °C			30 °C			50 °C			60 °C		
	<i>A</i>	<i>D_B</i>	<i>2D_C</i>									
DLPG	60.2	31.4	21.8	62.1	30.7	21.3	65.3	29.5	20.6	67.1	28.9	20.3
DMPG	NA			62.5	33.8	24.5	66.0	32.6	23.7	67.5	32.0	23.4
DPPG	NA			NA			64.7	36.7	27.8	66.8	35.9	27.2
DSPG	NA			NA			NA			66.8	39.1	30.4
POPG	62.5	38.5	29.2	64.3	37.6	28.6	68.4	36.1	27.6	69.6	35.7	27.4
SOPG	62.9	40.2	31.0	64.3	39.6	30.5	67.6	38.1	29.5	69.0	37.6	29.2
DOPG	67.9	37.1	28.5	69.1	36.6	28.2	71.1	36.0	27.9	71.7	35.9	27.8

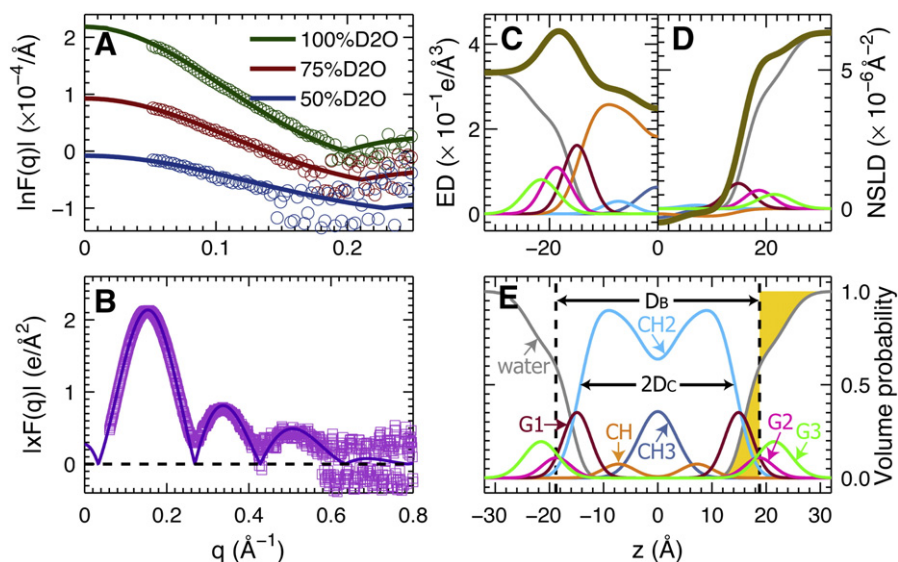


Fig. 3. SDP model analysis of a POPG lipid bilayer at 30 °C. (A) SANS data (symbols) at three D₂O concentrations and their associated fits (solid lines). For clarity, the 50% and 70% D₂O data are shifted downward by 0.5 and 1.0, respectively. (B) SAXS data (symbols) and the fit to the data (solid line). (C) and (D) are, respectively, the ED and NSLD (in 100% D₂O) profiles obtained from the best fits to SANS and SAXS data. The thick golden lines represent the total ED and NSLD in one bilayer leaflet. The color scheme for each component follows Fig. 1A. (E) Component volume probabilities. The hydrocarbon chain thickness 2D_c corresponds to the full width of the error function representing the sum of the CH, CH₂ and CH₃ components. The overall bilayer thickness D_B is defined by the Gibbs dividing surface (vertical dashed line), which separates the water distribution (yellow filled region) into two parts of equal areas.

was obtained between the scaled ED and vP. This indicates that a component's ED can be well represented by its vP. For more complete details regarding the SDP model, the reader is referred to the article by Kučerka et al. [24].

The parsing of the PG lipid used in the SDP model strongly depends on the lipid's chemical composition, which ultimately affects the scattering data. We first examined whether or not the previously developed SDP model [24] can be used to analyze SANS data from PG bilayers dispersed in aqueous solvent with different H₂O/D₂O ratios, *i.e.* when hydrogen/deuterium exchange is taking place. Fig. 1C compares bilayer component NSLD profiles to their corresponding vP distributions, with each NSLD scaled to its vP by the ratio of component's volume and neutron scattering length. For components that do not possess exchangeable hydrogens (*i.e.*, CH₃, CH₂, CH, G1 and G2), good overlap is obtained, with the exception of the backbone G1 whose NSLD and vP differ by 0.2 Å in the direction along the bilayer normal (*z* direction). This is because the backbone glycerol has three hydrogens, whereas the backbone carbonyl has none. Hydrogen's negative neutron scattering length shifts the maximum NSLD of G1 towards the carbonyl, which is located closer to the bilayer center. Note that the 0.2 Å difference for G1's NSLD and vP is always present, whether or not hydrogen exchange is taken into account.

The G3 component contains two hydroxyls with exchangeable hydrogens. Its NSLD therefore depends on the solvent's H₂O/D₂O ratio. For water compositions with 50, 70 and 100% D₂O (conditions used to obtain SANS data for all PG lipids [24,25]), the NSLDs of G3 are shown in the inset in Fig. 1C, along with its vP. It is clear that the G3 NSLD is well represented by its vP at all water compositions examined: the center and width of the NSLD are independent of the H₂O/D₂O ratio, and identical to the vP. This finding confirms that the previously developed SDP model [24] is suitable for reevaluating the data under conditions of hydrogen/deuterium exchange.

3. Results and discussion

3.1. Hydrogen exchange of headgroup glycerol hydroxyls

The PG lipid headgroup contains two OH groups, whose hydrogens exchange freely with the surrounding water. This was clearly shown

by NMR when only one characteristic OH peak was observed in mixtures formed by a hydroxy-compound and water [23]. Importantly however, exchange of hydrogen for deuterium has a profound effect on the NSLD of PG bilayers, which we illustrate in Fig. 2. In the case of 0% D₂O, two hydrogens are attached to the hydroxyl oxygens of the POPG headgroup (Fig. 2A, blue spheres). Increasing the D₂O concentration to 100% replaces the two hydrogens with two deuteriums (Fig. 2A, yellow spheres). The overall NSLD profiles of a POPG bilayer (water not included) with protiated and deuterated hydroxyls are shown in Fig. 2B. It is clear that hydrogen exchange with D₂O water not only increases the NSLD in the headgroup region, but also shifts the maximum NSLD away from the bilayer center. For water with a D₂O mole fraction *c* (0 ≤ *c* ≤ 1), the two PG hydroxyls on average possess 2*c* deuteriums and 2 × (1 − *c*) hydrogens. Failing to account for hydrogen exchange in the SDP analysis can affect the obtained structural parameters [26]. In the case of the PG headgroup, this results in an overestimation of lipid areas.

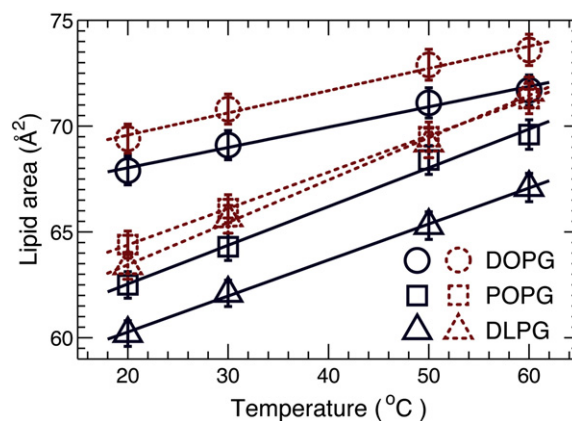


Fig. 4. The effect of hydrogen exchange on the lipid areas of DOPG, POPG and DLPG. Solid symbols and their linear fits (solid lines) were obtained from SDP analysis by taking into account exchangeable hydrogens, whereas the broken symbols and their linear fits (dashed lines) were obtained by omitting hydrogen exchange. Hydrogen exchange decreases the temperature-averaged lipid area by 1.7 Å² for DOPG, by 1.6 Å² for POPG, and by 3.8 Å² for DLPG.

3.2. Effect of hydrogen exchange on PG lipid bilayer structures

Using the previously developed SDP model [24] and accounting for hydrogen exchange of the PG hydroxyls, we reanalyzed the lipid bilayer structures of seven PG lipids (*i.e.*, DOPG, POPG, SOPG, DLPG, DMPG, DPPG and DSPG) at several temperatures. The obtained structural parameters are listed in Table 1. An example of the new SDP model fit is shown in Fig. 3 (POPG bilayer). The SDP model, which is described by component volume probabilities (Fig. 3E), was used to jointly refine three SANS datasets of different contrasts (Fig. 3A, symbols) and one SAXS dataset (Fig. 3B, symbols). The model curves (Fig. 3A and B, solid lines) were calculated from the Fourier transform of the bilayer ED (Fig. 3C) and NSLD (Fig. 3D) profiles, which were obtained by scaling the component volume probabilities with the corresponding electron numbers and neutron scattering lengths, respectively. Bilayer structural parameters such as hydrocarbon chain thickness $2D_C$, and overall bilayer thickness D_B are the same as in [24] (shown in Fig. 3E). Lipid area A is related to overall bilayer thickness D_B through the lipid's volume (V_L), $A = 2V_L / D_B$. A can also be calculated using the hydrocarbon chain volume and thickness, $A = (V_L - V_{HL}) / D_C$, where V_{HL} corresponds to PG's headgroup volume.

Fig. 4 shows lipid area results for three PG lipids (*i.e.*, the monounsaturated DOPG, the monounsaturated POPG and the disaturated DLPG lipid) using SDP analysis. The solid symbols were obtained by taking hydrogen exchange into account, while the dashed symbols correspond to our previous analysis, which omitted hydrogen exchange [25]. It is evident that the previous analysis overestimated lipid area by different amounts, depending on chain composition and temperature. In addition, the overestimation seems to be greater for the thinnest lipid bilayer, *i.e.*, DLPG. This is understandable, as the contribution of the headgroup hydroxyls to the overall bilayer NSLD becomes more pronounced with decreasing hydrocarbon chain length.

4. Conclusions

We have reanalyzed recently published fluid phase PG lipid bilayer data [24,25], this time taking into account the exchangeable OH hydrogens associated with the PG headgroup. Analysis of the data using the previously developed SDP model [24] shows that when exchangeable hydrogens are included, lipid areas for all PG lipids decrease. The temperature-averaged decrease is largest for the thinnest bilayer, DLPG (3.8 \AA^2), and smallest for the thickest bilayer, DSPG (1.5 \AA^2).

Acknowledgements

J.K. is supported through the Scientific User Facilities Division of the DOE Office of Basic Energy Sciences (BES), and by the Laboratory Directed Research and Development Program of Oak Ridge National Laboratory (ORNL), managed by UT-Battelle, LLC, for the U.S. Department of Energy (DOE) under contract no. DE-AC05-00OR2275. J.J.P. is partially supported by a startup fund from the University of South Florida.

Appendix A. Supplementary data

Supplementary data to this article can be found online at <http://dx.doi.org/10.1016/j.bbamem.2014.08.009>.

References

- [1] A.A. Spector, M.A. Yorek, Membrane lipid-composition and cellular function, *J. Lipid Res.* 26 (1985) 1015–1035.
- [2] J.H. Tong, J.T. Canty, M.M. Briggs, T.J. McIntosh, The water permeability of lens aquaporin-0 depends on its lipid bilayer environment, *Exp. Eye Res.* 113 (2013) 32–40.
- [3] T.J. McIntosh, S.A. Simon, Roles of bilayer material properties in function and distribution of membrane proteins, *Annu. Rev. Biophys. Biomol. Struct.* 35 (2006) 177–198.
- [4] G.W. Feigenson, Phase diagrams and lipid domains in multicomponent lipid bilayer mixtures, *Biochim. Biophys. Acta Biomembr.* 1788 (2009) 47–52.
- [5] J.F. Nagle, S. Tristram-Nagle, Structure of lipid bilayers, *Biochim. Biophys. Acta Rev. Biomembr.* 1469 (2000) 159–195.
- [6] W. Rawicz, K.C. Olbrich, T. McIntosh, D. Needham, E. Evans, Effect of chain length and unsaturation on elasticity of lipid bilayers, *Biophys. J.* 79 (2000) 328–339.
- [7] J. Henriksen, A.C. Rowat, E. Brief, Y.W. Hsueh, J.L. Thewalt, M.J. Zuckermann, J.H. Ipsen, Universal behavior of membranes with sterols, *Biophys. J.* 90 (2006) 1639–1649.
- [8] Y.W. Hsueh, M.T. Chen, P.J. Patty, C. Code, J. Cheng, B.J. Frisken, M. Zuckermann, J. Thewalt, Ergosterol in POPC membranes: physical properties and comparison with structurally similar sterols, *Biophys. J.* 92 (2007) 1606–1615.
- [9] B.W. Koenig, H.H. Strey, K. Gawrisch, Membrane lateral compressibility determined by NMR and X-ray diffraction: effect of acyl chain polyunsaturation, *Biophys. J.* 73 (1997) 1954–1966.
- [10] D. Huster, K. Arnold, K. Gawrisch, Investigation of lipid organization in biological membranes by two-dimensional nuclear overhauser enhancement spectroscopy, *J. Phys. Chem. B* 103 (1999) 243–251.
- [11] H.I. Petrache, S.W. Dodd, M.F. Brown, Area per lipid and acyl length distributions in fluid phosphatidylcholines determined by ^2H NMR spectroscopy, *Biophys. J.* 79 (2000) 3172–3192.
- [12] A.R. Braun, E.G. Brandt, O. Edholm, J.F. Nagle, J.N. Sachs, Determination of electron density profiles and area from simulations of undulating membranes, *Biophys. J.* 100 (2011) 2112–2120.
- [13] S. Shenoy, R. Moldovan, J. Fitzpatrick, D.J. Vanderah, M. Deserno, M. Losche, In-plane homogeneity and lipid dynamics in tethered bilayer lipid membranes (tBLMs), *Soft Matter* 6 (2010) 1263–1274.
- [14] M. Mihalescu, R.G. Vaswani, E. Jardon-Valadez, F. Castro-Roman, J.A. Freites, D.L. Worcester, A.R. Chamberlin, D.J. Tobias, S.H. White, Acyl-chain methyl distributions of liquid-ordered and -disordered membranes, *Biophys. J.* 100 (2011) 1455–1462.
- [15] E.G. Brandt, A.R. Braun, J.N. Sachs, J.F. Nagle, O. Edholm, Interpretation of fluctuation spectra in lipid bilayer simulations, *Biophys. J.* 100 (2011) 2104–2111.
- [16] M.C. Wiener, S.H. White, Fluid bilayer structure determination by the combined use of X-ray and neutron-diffraction. I. Fluid bilayer models and the limits of resolution, *Biophys. J.* 59 (1991) 162–173.
- [17] G. Pabst, N. Kučerka, M.P. Nieh, M.C. Rheinstadter, J. Katsaras, Applications of neutron and X-ray scattering to the study of biologically relevant model membranes, *Chem. Phys. Lipids* 163 (2010) 460–479.
- [18] P. Heftberger, B. Kollmitzer, F.A. Heberle, J.J. Pan, M. Rappolt, H. Amenitsch, N. Kučerka, J. Katsaras, G. Pabst, Global small-angle X-ray scattering data analysis for multilamellar vesicles: the evolution of the scattering density profile model, *J. Appl. Crystallogr.* 47 (2014) 173–180.
- [19] T.T. Mills, G.E.S. Toombes, S. Tristram-Nagle, D.M. Smilgies, G.W. Feigenson, J.F. Nagle, Order parameters and areas in fluid-phase oriented lipid membranes using wide angle x-ray scattering, *Biophys. J.* 95 (2008) 669–681.
- [20] W.C. Hung, M.T. Lee, F.Y. Chen, H.W. Huang, The condensing effect of cholesterol in lipid bilayers, *Biophys. J.* 92 (2007) 3960–3967.
- [21] G. Pabst, M. Rappolt, H. Amenitsch, P. Laggner, Structural information from multilamellar liposomes at full hydration: full q-range fitting with high quality x-ray data, *Phys. Rev. E* 62 (2000) 4000–4009.
- [22] F.A. Heberle, J.J. Pan, R.F. Standaert, P. Drazba, N. Kučerka, J. Katsaras, Model-based approaches for the determination of lipid bilayer structure from small-angle neutron and X-ray scattering data, *Eur. Biophys. J.* 41 (2012) 875–890.
- [23] I. Weinberg, J.R. Zimmerman, Concentration dependence of chemical exchange and NMR multiplet structure in water–ethanol mixtures, *J. Chem. Phys.* 23 (1955) 748–749.
- [24] N. Kučerka, B.W. Holland, C.G. Gray, B. Tomberli, J. Katsaras, Scattering density profile model of POPG bilayers as determined by molecular dynamics simulations and small-angle neutron and X-ray scattering experiments, *J. Phys. Chem. B* 116 (2012) 232–239.
- [25] J.J. Pan, F.A. Heberle, S. Tristram-Nagle, M. Szymanski, M. Koepfinger, J. Katsaras, N. Kučerka, Molecular structures of fluid phase phosphatidylglycerol bilayers as determined by small angle neutron and X-ray scattering, *Biochim. Biophys. Acta Biomembr.* 1818 (2012) 2135–2148.
- [26] J.J. Pan, X.L. Cheng, L. Monticelli, F.A. Heberle, N. Kučerka, D.P. Tieleman, J. Katsaras, The molecular structure of a phosphatidylserine bilayer determined by scattering and molecular dynamics simulations, *Soft Matter* 10 (2014) 3716–3725.